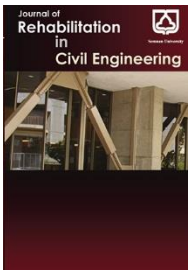

journal homepage: http://civiljournal.semnan.ac.ir/

Assessing Seismic Performance of the Elliptic Braced Moment Resisting Frame through Pushover Method

H. Ghasemi Jouneghani[1*], A. Haghollahi[2], H. Moghaddam[3] and A. Sarvghad Moghadam[4]

1. PhD Candidate, Department of Civil Engineering, Shahid Rajaee Teacher Training University, Tehran, Iran.
2. Assistant Professor, Department of Civil Engineering, Shahid Rajaee Teacher Training University, Tehran, Iran.
3. Professor, Department of Civil Engineering, Sharif University, Tehran, Iran.
4. Associate Professor, International Institute of Earthquake Engineering and Seismology (IIEES), Tehran, Iran.

Corresponding author: *haghollahi@srttu.edu*

ARTICLE INFO

Article history:
Received: 08 November 2017
Accepted: 05 February 2018

Keywords:
Elliptic Braced Moment,
Resisting Frame,
Nonlinear Static Pushover,
Analysis,
Seismic Performance,
Response Modification Factor,
Overstrength Factor,
Ductility Factor,
Plastic hinges.

ABSTRACT

The seismic performance of elliptic braced moment resisting frame (ELBRF) is assessed here and is found that the structural behavior is improved and is of free of architectural space. The demand for seismic performance of ELBRF is estimated through conventional pushover methods of 3, 5, 7, and 10-story ELBRF frames and they are compared with special moment resisting frames (SMRF) and X-Braced CBF and Inverted V-Braced CBF concentrically braced frames. The effective parameters in the seismic design of structures, like the ductility, overstrength and response modification factors are evaluated. The response modification factor for ELBRF in the design by ultimate limit state and allowable stress methods is proposed as 10 and 14.4, respectively. Finally, the process of forming plastic hinges in ELBRF is assessed and it is found that an increase in height makes the plastic hinges to be transmitted to the upper stories, allowing the structure to collapse at higher stories.

1. Introduction

Studying the destruction of buildings during earthquakes reveals that the conventional elastic methods are ineffective in the building design. These methods do not provide a real insight on how structures behave when exposed to the extreme seismic phenomenon. The real performance of structures is determined through performance-oriented methods and guidelines subject to a new outstanding design approach named performance-based design [1]. This new analytical design method has two major differences comparing to the conventional perspectives of earthquake engineering, that is, first, direct relation between design and structural performance, second, multiple

DOI: 10.22075/JRCE.2018.13030.1232

functionality. The performance targets may be a level of stress not to be exceeded a load, a displacement, a limit state or a target damage state.

The proposed seismic design systems emphasize on performance-based seismic design (PBSD) concept to have a more realistic assessment on the inelastic response of the structure [2]. According to [3] most of the available seismic design methods are still based on elastic analysis approach for assessing the inelastic behavior. Consequently, the current performance-based design methodology relies heavily on an iterative "Assess Performance and Revision Design", to achieve a design procedure which is capable to accomplish the intended objectives.

Both structural and nonstructural damages occurred during ground motions due to earthquake are primarily produced by lateral displacements. Therefore, estimating lateral displacement is of essence in the performance-based earthquake resistant design, especially when the damage control volume is of concern. However, there are many uncertainties associated with the generation of site-specific input and with the analytical models presently employed to represent structural behavior [4]. In many cases, making efforts in detailed analysis and modeling may not be possible; therefore, it is safer to be aware of having a simpler tool for analyzing seismic performance of a frame structure [5].

Although nonlinear dynamic method [6,7] is commonly applied in theoretical studies, it is time-consuming and often difficult to be applied in designing, it is worth applying a simple analysis method to evaluate the seismic performance of the structure. Nonlinear Static Pushover Analysis (NSPA) is the appropriate method for this purpose [8]. Very important information can be obtained from a simple and cost-effective NSPA method, rather than running dynamic analysis.

Nowadays, concentric and eccentric bracings are the most common types of bracing systems applied in design and strengthening structures against seismic lateral loads, while they cause problems in providing the required space to create an opening in the building walls [9]. Consequently, a modern structural form is proposed in this article, which would lead to higher efficiency in the design and architecture through an elliptic brace in the middle opening of a frame in a manner that the ELBRF system is free of the common architectural space problem of an opening in introducing the bracing system [10].

In this study, the frames were designed based on the Iranian code of practice for seismic resistance design of buildings [11] and Iranian National Building Code for Steel Structural Design [12]. Here, the nonlinear static pushover analysis is run to accomplish the objectives. The ELBRF system is a new lateral load system which can be analyzed through these methods. ELBRF has more advantages over other structural systems in terms of performance [10].

The objective of this article is to evaluate the seismic performance of ELBRF system based on FEMA-356 load patterns (2000) [13], a pushover modal analysis and to compare it with other structural systems, like special moment resisting frames (SMRF), X-Braced CBF and Inverted V-Braced CBF concentrically braced frames.

The effective parameters in the seismic design of the braced steel structures: like the ductility, overstrength and response modification factors in ELBRF are calculated and compared with SMRFs, X-Braced CBF and Inverted V-Braced CBF. The process of forming plastic hinges in ELBRF frames is assessed and compared with other structural systems.

2. Elliptic Bracing System

The SMRF and concentrically braced frame (CBF) are normally applied in structures with the objective to make them resist and transfer gravitational and lateral loads of wind and earthquake. Structures with SMRF subject to lateral load generate appropriate structural plasticity [14,15]. If such a structure is designed, application of essential parameters like the excessive relative displacement due to high flexibility of the structure and the inevitable stress concentration at the welding of columns and beams constrain the utility of the structures. The improved stiffness, in order to reduce the excessive structural deformation can be achieved by applying (CBF). When bracing parts are added to SMRF system, despite a reduction in stiffness, lower ductity of CBF would prevent the implementation of such a design because the seismic performance is an important factor [9,16].

It is revealed in previous studies that bracing members' buckling in CBF would undergo considerable structural defaults, strength and promote energy loss [17,18].

Where ELBRF as a new proposed structural form is applied in the intermediate opening of the frame, design efficiency would be increased. The elliptic brace, due to providing a broader architecture as to opening is better than concentric bracing. Applying this newly proposed ELBRF, in addition to improving structure behavior and energy dissipation there of it opening space is free of architectural space problem [10]. An example of elliptic brace is shown in Fig. 1.

In ELBRE system the beam and column connections to the elliptic brace connections, thereof are assumed to be clamped as double joints, that is, the connections must have sufficient flexural stiffness at the connection point to withstand out-of-plane buckling. In these circumstances, the braces of the truss parts are not perpendicular to the frame plate, rather act as beam-column elements. Bracings under pressure might experience out-of-plane buckling caused by generated deformations at beam and column connection points in the plate frames, Fig. 2. In addition, the braces could be designed and installed if appropriate bracing connections are available on the beam and column, which would provide sufficient stiffness [10].

3. Nonlinear Static Procedures for Seismic Demand Estimation

In a Nonlinear Static Pushover Analysis (NSPA) or pushover analysis in the NEHRP guidelines [13, 19], the seismic requirements are calculated through static nonlinear analysis of the structure exposed to a steady increase in lateral forces with an invariant constant height distribution, to a point where the displacement of a particular point (control point) reaches a specified target displacement rate or cause structure collapse. The essential requirement for pushover analysis is to choose the appropriate lateral load pattern. The correlation between story drift and the applied load pattern is critical [20]. The load pattern applied to the structure in the analysis represents the distribution of

the inertial force at the structure height which is inflicted during the earthquake. Selecting a model more proportional and similar to inertial forces distribution would yield to better results in analyses [21]. In this article the inverted triangular load pattern, uniform load pattern, mode one load pattern and Modal Pushover Analysis (MPA) are applied [22,23] according to FEMA-356 (2000) [13].

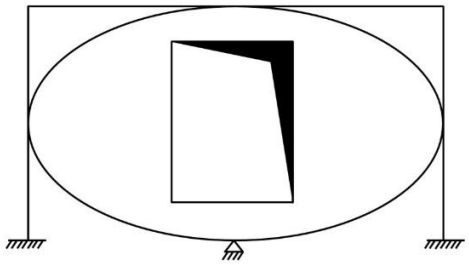

Fig. 1. Frame with elliptic bracing [10].

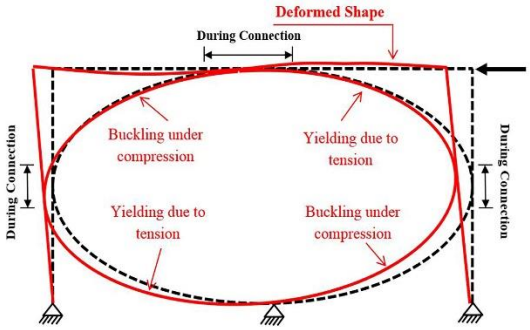

Fig. 2. Nonlinear deformation in elliptic bracing [10].

4. Calculating Response Modification Factor

There exist several methods through which the response modification factor is calculated. The most notable method among them is the ductility factor developed by [24], where, the actual nonlinear behavior of a structure is equivalent to a bilinear ideal curve (Idealized Response). To illustrate this, the hardness of the super-algebra section is approximated based on the approximate equilibrium of the surfaces with a line. Effective elastic hardness is plotted by a transient lane from a point on the capacity curve in accordance with a 0.6Vy cut [24].

In the mentioned graph, Vy is the yielding force and Ve is the maximum base shear when behavior of the structure is assumed to be linear during an earthquake. Ve is reduced to Vy due to the ductility and nonlinear behavior of the structure, Fig. 3.

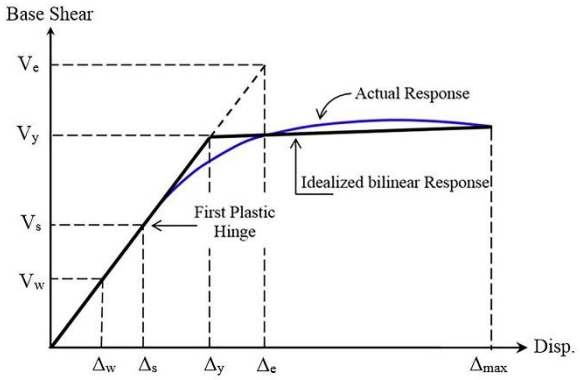

Fig. 3. Nonlinear behavior of structure.

Response modification factor is applied to convert the linear force of the structure in to design force. Thus, Eqs. (1 and 2) are applied in a given design where the allowable stress and ultimate resistance methods respectively are of concern, respectively [24]:

$$R = (V_e/V_y) \times (V_y/V_s) \times (V_s/V_w) = R_\mu \times R_s \times \gamma \quad (1)$$

$$R = (V_e/V_y) \times (V_y/V_s) = R_\mu \times R_s \quad (2)$$

where, R_μ is the force reduction factor and γ is the allowable stress factor. Here, the allowable stress factor is considered as 1.44, based on UBC-97 recommendations [25]. Overstrength factor is the base shear of mechanism formation (Vy) to base shear of the first hinge formed in the structure (Vs) ratio, after the first yield in the elements, defined as follows [24]:

$$R_s = V_y/V_s$$

This factor is based on the nominal specifications of materials, named RSO. Some other effects are considered in the real overstrength factor (Rs), defined as follows [24]:

$$R_s = R_{SO} \times F_1 \times F_2 \ldots . F_n$$

where, F is the difference between the actual and nominal static yield strengths and F2 indicates the increased yield stress caused by the strain rate during an earthquake. In this article, both the F1 and F2 are considered to be 1.15 as recommended by both the references [24], and Iranian National Building Code for Steel Structural Design [12].

5. The Studied Models

In this study, 4 frames are designed through SMRFs, X-Braced CBF, Inverted V-Braced CBF and ELBRF systems according to the requirements of Iranian code of practice for seismic resistance design of buildings [11] and Iranian National Building Code [12] for 3, 5, 7, and 10-stories for steel structures, which are assumed to be in an area with high seismicity set on type II soil with the average shear wave velocities of 360-750 m/s squared at a depth of 30 m [11].

The height of all stories is 3 meters, the spans are 3 with 6 Meters length. The mid-span of the frames is braced. The location of the braces is presented in dotted line in Fig. 4. The weight effects of the other frames are modeled by a dummy column, Fig. 4. Type ST37-1 steel (equal to S235 steel based on EN 10025 standard) and a yield stress of 235 MPa is used. The dead and live loads are equal to 5.0 and 2.0 KN/m2, respectively. All connections, including those of the beam-to-column and brace-to-beam and brace-to-column are clamped. All the supports of the columns are clamped in a manner where any translational and rotational degrees of freedom are constant and the supporting conditions are expected to occur in the middle of the frames beneath the elliptic bracings in the forms of hinged supports forms.

The equivalent static lateral forces on all the stories are applied in designing the SMRF, X-Braced CBF, Inverted V-Braced CBF and ELBRF subject to the earthquake effect. These forces are calculated based on Iranian code of practice for seismic resistance design of buildings [11]:

$$V = C.W = [(A \times B \times I)/R].W$$

where, V is the base shear, C is the seismic coefficient, W is the effective structural weight, A is the design base acceleration, B is the response factor, I is the importance rate and R is the response modification factor (behavior ratio). The Importance Factor (I) and the design base acceleration (A) of the frames are 1 and 0.35, respectively.

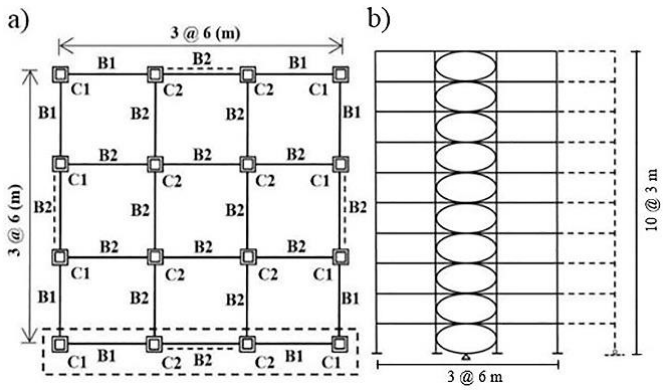

Fig. 4. Configuration of model structure by Open Sees. (a) Plane. (b) Brace configuration with dummy column.

Table 1. Cross sections of ELBRF model members.

Frame		ELBRF			
Structures	Story	C1 (BOX)	C2 (BOX)	B1&2 (IPE)	Brace (BOX)
3 - Story	1	200×20	200×20	360	100×10
	2	150×15	200×20	360	100×10
	3	150×15	150×10	330	100×10
5 - Story	1	200×20	200×20	330	100×10
	2	200×20	200×20	330	100×10
	3	200×20	200×20	330	100×10
	4	150×20	150×20	330	100×10
	5	150×10	150×10	330	100×10
7 - Story	1	250×20	250×20	400	120×12
	2	250×20	250×20	400	120×12
	3	250×20	250×20	400	120×12
	4	250×20	250×20	360	120×12
	5	200×20	200×20	360	100×10
	6	200×20	200×20	330	100×10
	7	200×20	200×20	330	100×10
10 - Story	1	350×30	350×30	450	120×12
	2	350×30	350×30	450	120×12
	3	350×30	350×30	400	120×12
	4	350×30	350×30	400	120×12
	5	350×30	350×30	400	120×12
	6	250×25	250×25	400	120×12
	7	250×25	250×25	360	100×10
	8	200×20	200×20	360	100×10
	9	200×20	200×20	330	100×10
	10	200×20	200×20	330	100×10

The response modification factor for SMRF, X-Braced CBF, Inverted V-Braced CBF and ELBRF in ultimate limit state design method is 7.5, 7.0, 7.0 and 9.0, respectively. Some parts of the frame are designed based on the Iranian National Building Code for Steel Structural Design [12] by applying Load and Resistance Factor Design (LRFD). The cross-sections of model members are shown in Table 1.

In order to reduce the time and cost of the calculations in NSPA, a two-dimensional frame is selected as the three-dimensional structure representative.

6. OpenSees Software

6.1. Modeling Process

OPENSEES 2.4.6 version [26] has been and is being applied in modeling structures and run NSPA. This software, developed by Berkeley University of California, is one of the most effective software for nonlinear analysis.

In this study, to model members in the of nonlinear deformations range, the following items are of major concern:

Structure designe in 3D in ETABS software

Structure frame selection in a 2D environment in OPENSEES 2.4.6 [26]

Structure, loading and seismic force on the xz plane in 2D and masses of the floor placed on the levels of the story

Elastic modeling of beam and column members of the frame, concentrated plastic hinges (CPH) of the column at both ends and the concentrated plastic hinges (CPH) of the beam at 10% of the length at its both ends

Installation of plastic hinges at the middle span of the frame at the junction of the elliptic brace to the beam and column - in the middle of the span of the beam and the column

Installation of four plastic hinges at every quarter of the length of the elliptic brace and installation of shear panels at beam and column junction

The schematic configuration of these items are shown in Fig. 5.

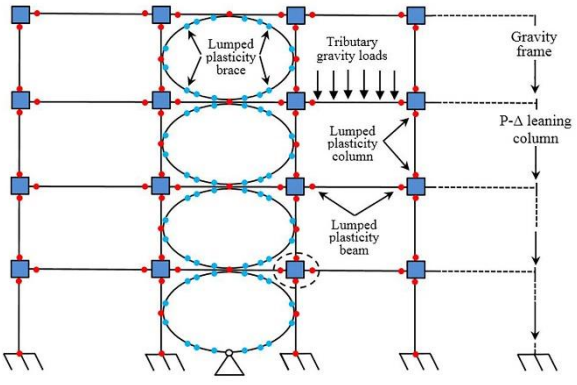

Fig. 5. Schematic configuration of centralized plastic hinges and shear panels in the ELBRF frame.

The effect of other frames' weights is modeled through a dummy column. To model the P-Δ effect of adjacent gravity

frames, a dummy column connected with truss elements to the main frame is applied. The dummy column is applied to half the gravity columns of 3D structure P-Δ effect, where the moment of inertia and cross-section of which is 100 times greater than the main frame columns [27]. The dummy column is connected to each dummy column of the upper story at each story with a spring of zero-length element with a slight resistance is to provide a slight flexural strength. The truss elements are located between the main frame and the dummy column and transfer the of dummy column P-Δ effect to the main frame. Half of the gravity frames' loads adjacent to each story are placed on the dummy column node at the given level. The area of the truss elements are 100 times greater than that of the main frame beams and they are assumed to be rigid in terms of axial strength. The bottom of the dummy column is considered as a hinge.

Conversion of the coordinates of the columns and beams is adopted by P-delta and linear methods, respectively. Flexibility of the foundation is ignored, and the bottom of the columns are clamped. To model a rigid diaphragm, the horizontal displacement of all nodes in a story is tightened to the first left node on the same story with respect to the equal DOF command. Half of the total mass of each story is assigned to 2D frame nodes at the same level.

To model bracing elements in braced moment X-Braced CBF and Inverted V-Braced CBF frames, the bracing member is considered as a wide plasticity and force-based elements with fiber sections are applied concentric manner, Fig. 6.

The P-delta effects and non-linear geometric deformations are considered through the corotational deformation of the geometric stiffness matrix type in the program [26]. A nonlinear beam-column element is applied to model braces to account for the effects of moderate to large deformations due to nonlinear buckling of members. Through this element the effects of P- Δ and large deformations of the non-linear geometric effect can be considered in the model. In order to increase the accuracy of the analysis in modeling the structure, five integration points assigned to the model. Bracing members in Braced CBF and Inverted V-Braced CBF structures are of two sections and the initial defect in the mid area at 0.002 of member length is assigned to nonlinear geometric consideration. To model steel material in this case, Steel02 were used, Fig. 7. To model the steel material failure, the strains are limited by applying MinMax materials. The tensile strength of the steel is considered at 2% in the elastic zone.

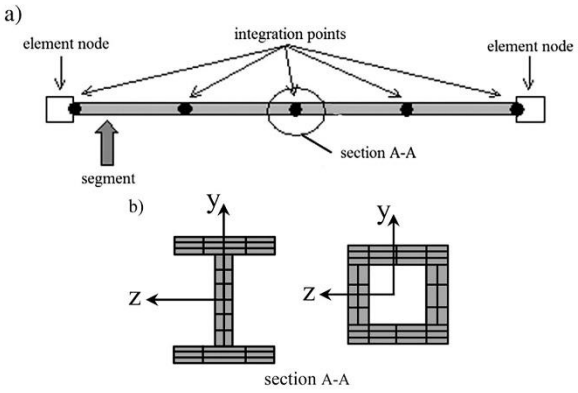

Fig. 6. Schematic division of element and section into segment and fiber elements in OpenSees:

a) Dividing the element into several segments,
b) Dividing the section into fiber elements [26]

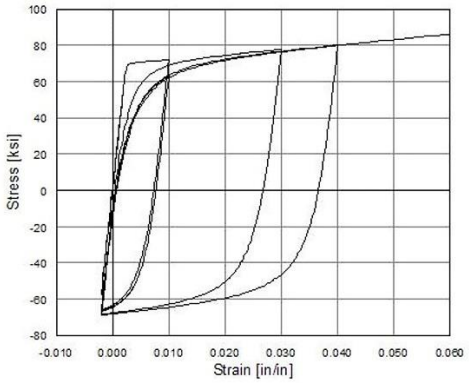

Fig. 7. Nonlinear deformation in elliptic bracing [26].

6.2. Modeling the Panel Zone and the Concentrated Plastic Hinges

A typical moment frame consists mainly of columns, beams, panel zone, and beam-to-column connections. The analytical modeling techniques found in SMRF are classified according to the linear or nonlinear behavior of structural components or by considering or ignoring the dimensions of the connection areas. Because SMRFs have always been and are trusted as one of the flexible lateral load systems with the ability to withstand large nonlinear deformations, precise modeling of beam-to-column connections and panel zones may be considered as important as the beams and columns modeling [28]. In nonlinear analytical models consisting of panel zones, are included in a panel zone model which is applied between rigid bodies and a nonlinear spring, presented by Krawinkler [29]. This parallelogram model describes a more accurate representation of the real behavior of the panel zone, while, increasing the complexities of the model in a significant manner.

In this model, nonlinear behavior is reflected through the concentrated ductility in rotational spring's concept. The inelastic springs in beams and columns are modeled through the peak oriented Ibarra element model [30] where the hysteretic deterioration and the negative stiffness of the element within the cycle are of concern, thus causing the structure collapse. For each one of the beams and columns, the yield point of the model with the plastic flexural strength for the section, MP is calculated with the expected values for the steel yielding strength, (e.g., 1.1Fy is defined). The initial rotational stiffness of the column is based on the Young's modulus for steel material and the cross-sectional stiffness. Calculating beam stiffness involves the share from the composite floor slab. The rotational behavior of the plastic regions in the models follows a bilinear hysteretic response based on the modified Ibarra Krawinkler deterioration model [31,32].

The SMRF is modeled through the elastic beam-column elements joined by the Zero Length elements where, the rotational spring application exhibit the nonlinear behavior of the structures. Based on the modified Ibarra Krawinkler deterioration model the springs are subject to bilinear hysteretic response [33].

In this study a parallelogram model is adopted to illustrate the shear behavior of panel zone. The shear distortion - the uniform shear force correlation proposed by Krawinkler [29] - is demonstrated in Fig. 8. The boundary elements applied in the model are of rigid beam-column element with a high axial and flexural stiffness type in the form of a parallelogram with depth of beam (db) in depth of column (dc) dimensions. The shear strength and stiffness of the panel zone can be modeled by providing a three-line rotational spring in each one of the corners, Fig. 8. To verify the authenticity of the panel zones constructed in the OpenSees software [26], the panel zones are modeled through a

combination of available standard beam-column and the flexural spring modules. One of the most influential models that fully describes the deterioration mode is introduced by [34], where energy dissipation in each cycle is considered as deterioration criterion and can be modeled together with any of the three general linear residue models, (e.g. applying a direct bilinear model, a peak-oriented model and or modeling a pinching model). The original proposed model by [35,36] is modified mainly for steel parts. These modifications are complementary to the definitions and simulations of deterioration, Fig. 9.

Since a frame member is modeled as a connected elastic element of rotational springs in a series at its ends, the stiffness of these components must be modified in a sense that the stiffness of this assembly is equivalent to the stiffness of the real frame member. By adopting the method described in Appendix B introduced by [27], the rotational springs should be "n" times stiffer than the elastic element's rotational stiffness (n=10) to prevent numerical problems and attribute all damping thereof, to the elastic element. To assure that the assembly stiffness and real frame member stiffness equilibrium the stiffness of this elastic element should be "(n + 1) / n" times more than the stiffness of the real frame member. This is accomplished by increasing of the moment inertia of the elastic elements in relation to the moment inertia of the real frame elements by "(n+1)/n" times [27].

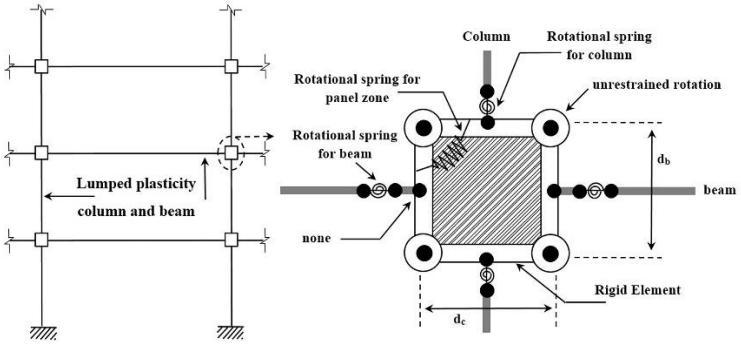

Fig. 8. Modeling of structural components in moment-resisting frames [37].

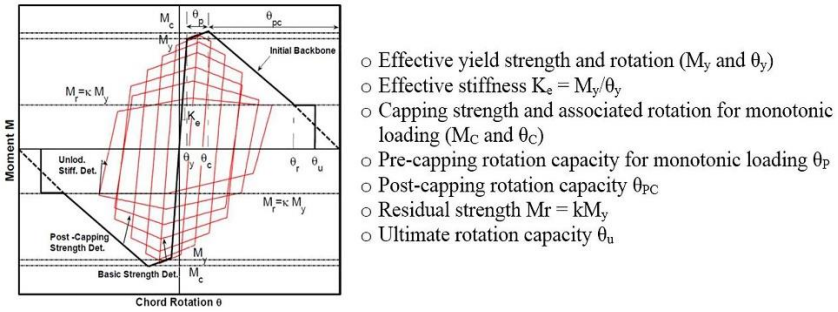

Fig. 9. Backbone curve of the modified Ibarra-Krawinkler model [35,36].

6.2.1. Yield Strength and Elastic Stiffness of the Panel Zone

The following multi-equations are applied in calculating the Yield Strength of the Panel Zone and the Elastic Stiffness of the Panel Zone [38]:

$$V_y = \frac{F_y}{\sqrt{3}} A_{eff} = \frac{F_y}{\sqrt{3}} (0.95 d_c t_p) \approx 0.55 F_y d_c t_p$$

where, Vy is the panel zone shear yield strength, Fy is the material yield strength, Aeff is the effective shear area, dc is the depth of the column, and tp is the thickness of the web including any doubler plates. The corresponding yield distortion, γy, is expressed as: $\gamma_y = F_y/(\sqrt{3} \times G)$. where, G is the shear modulus of the column material.

The elastic stiffness, Ke, of the panel zone can then be written as: $K_e = \frac{V_y}{\gamma_y} = 0.95 d_c t_p G$.

By considering Fy, ES, G and γy are respectively 2.35E + 08, 2.00E + 11, 1.30E + 11 and 1.05E-03, the elastic stiffness of the panel zones are tabulated in Table 2.

6.2.2. The specifications of plastic hinges for beams, columns and braces

To calculate the correlation regarding plastic hinges of the beams the W-section equation and together with the other-than-RBS beam sections provided by [36] are applied. In the modeled sections in [36], d <533 (mm) the specifications of plastic hinges of the beams are tabulated in Table 3. The Hollow Square tube sections equation provided by [36,39] is applied to calculate the behavior of the plastic hinges of the columns and elliptic braces with box section. According to [36,39] and with respect to 20 <D / t <40, 0 <N / Ny <0.40 and 40 <Fy <66.5 (ksi), the specifications of the plastic hinges of the columns are tabulated in Table 4.

The brace sections are hollow and square in shape. Because there exists a significant axial force in the bracing system, the equations related to the columns are applied.

The value of force-to-capacity parameter in calculating the parameters of the central hinges of the columns and braces vary. The plastic hinge specifications of braces are tabulated in Table 5. To match the nonlinear behavior of the model made through the main frame members, the hardening factor (stiffness before yielding to elastic stiffness ratio) of the plastic hinges should be modified. If the hardening factor of the main frame members is considered as αs,mem, the hardening factor of the torsional springs (plastic hinge point) would equal to αs, spring = αs, mem / (1 + n * (1 - αs, mem)) [27].

Table 2. Yield Strength Elastic Stiffness and of Panel Zone.

dc	tp	Aeff	Vy	Ke
0.45	0.03	2.61E-02	3.55E+06	3.39E+09
0.4	0.03	2.31E-02	3.14E+06	3.00E+09
0.35	0.03	2.01E-02	2.73E+06	2.61E+09
0.3	0.03	1.71E-02	2.32E+06	2.22E+09
0.3	0.025	1.44E-02	1.95E+06	1.87E+09
0.3	0.02	1.16E-02	1.58E+06	1.51E+09
0.25	0.025	1.19E-02	1.61E+06	1.54E+09
0.25	0.02	9.60E-03	1.30E+06	1.25E+09
0.2	0.025	9.38E-03	1.27E+06	1.22E+09
0.2	0.02	7.60E-03	1.03E+06	9.88E+08
0.15	0.02	5.60E-03	7.61E+05	7.28E+08
0.15	0.01	2.90E-03	3.94E+05	3.77E+08
0.15	0.015	4.28E-03	5.81E+05	5.56E+08
0.15	0.025	6.88E-03	9.34E+05	8.94E+08
0.1	0.01	1.90E-03	2.58E+05	2.47E+08

7. The Analytical Results

7.1. Nonlinear Static Analysis

Non-linear static analysis is run and the Roof displacement-base shear diagrams related to

the ELBRF for 3, 5, 7 and 10-story structures is plotted through the results obtained from OPENSEES software [26] for the inverted triangular load pattern and the uniform load pattern and with SMRFs, X-Braced CBF and Inverted V-Braced CBF concentrically braced frames are compared, Fig. 10. The values of the static base shear corresponding to the formation of the first plastic hinge in the SMRF, X-Braced CBF, Inverted V-Braced CBF and ELBRF structures for different stories are tabulated in Table 6.

Table 3. Specifications of the plastic hinges of beams.

Beam Section	h (mm)	t_w (mm)	b_f (mm)	t_f (mm)	d (mm)	L (mm)	F_y (MPa)	M_y (N.mm)	M_C =1.27M_y	θ_P	θ_{PC}	Λ
IPE 300	248	7.1	150	10.7	300	5400	235.4	16.25 E+07	20.63 E+07	0.071	0.20	1.43
IPE 330	271	7.5	160	11.5	330	5400	235.4	20.81 E+07	26.42 E+07	0.071	0.20	1.43
IPE 360	298	8.0	170	12.7	360	5400	235.4	26.38 E+07	31.65 E+07	0.065	0.21	1.45
IPE 400	331	8.6	180	13.5	400	5400	235.4	29.94 E+07	38.02 E+07	0.057	0.20	1.39
IPE 450	378	9.4	190	14.6	450	5400	235.4	44.06 E+07	55.95 E+07	0.050	0.20	1.33
IPE 500	426	10.2	200	18.0	500	5400	235.4	56.80 E+07	72.14 E+07	0.045	0.21	1.39

In the Table above:

h = web depth, tw= web thickness, bf = wide flange, tf = flange thickness, d = beam depth, L/d =span-to-depth ratio, Fy = expected yield strength of the flange of the beam in megapascals (Fy= 235 MPa), θP= pre-capping plastic rotation for monotonic loading (difference between yield rotation and rotation at maximum moment), θPC = post-capping plastic rotation (difference between rotation at maximum moment and rotation at complete loss of strength), $\Lambda = \lambda \cdot \theta$ = reference cumulative rotation capacity.

Table 4. Specifications of the plastic hinges of columns.

D (mm)	t (mm)	θ_P	θ_{PC}	My (N.mm)	M_C = 1.27My	Λ	N/Ny
450	30	0.028	0.159	20.58 E+08	24.90 E+08	1.856	0.4
400	30	0.031	0.184	15.98 E+08	19.34 E+08	2.490	0.4
350	30	0.036	0.216	11.96 E+08	14.47 E+08	3.473	0.4
300	30	0.042	0.261	85.28 E+07	103.19 E+07	5.099	0.4
300	25	0.035	0.209	73.62 E+07	89.08 E+07	3.237	0.4
300	20	0.028	0.159	60.99 E+07	73.80 E+07	1.856	0.4
250	25	0.042	0.261	49.35 E+07	59.71 E+07	5.099	0.4
250	20	0.033	0.199	41.19 E+07	49.84 E+07	2.924	0.4
200	25	0.053	0.343	29.93 E+07	36.22 E+07	8.892	0.4
200	20	0.042	0.261	25.26 E+07	30.56 E+07	5.099	0.4
150	25	0.070	0.486	15.37 E+07	18.60 E+07	18.212	0.4
150	20	0.056	0.371	13.22 E+07	16.00 E+07	10.444	0.4
150	15	0.042	0.26	10.66 E+07	12.89 E+07	5.100	0.4
150	10	0.028	0.159	76.24 E+06	92.25 E+06	1.856	0.4
100	10	0.042	0.261	31.58 E+06	38.21 E+06	5.099	0.4

Table 5. Specifications of the plastic hinges of columns.

D (mm)	t (mm)	θ_P	θ_{PC}	My (N.mm)	M_C = 1.27My	Λ	N/Ny
120	12	0.0511	0.399	54.45 E+06	65.88 E+06	8.748	0.3
100	10	0.0511	0.399	31.58 E+06	38.21 E+06	8.748	0.3

In the Table above: D = section depth, t = thickness of box section, N = the applied axial load, Ny = the yield load.

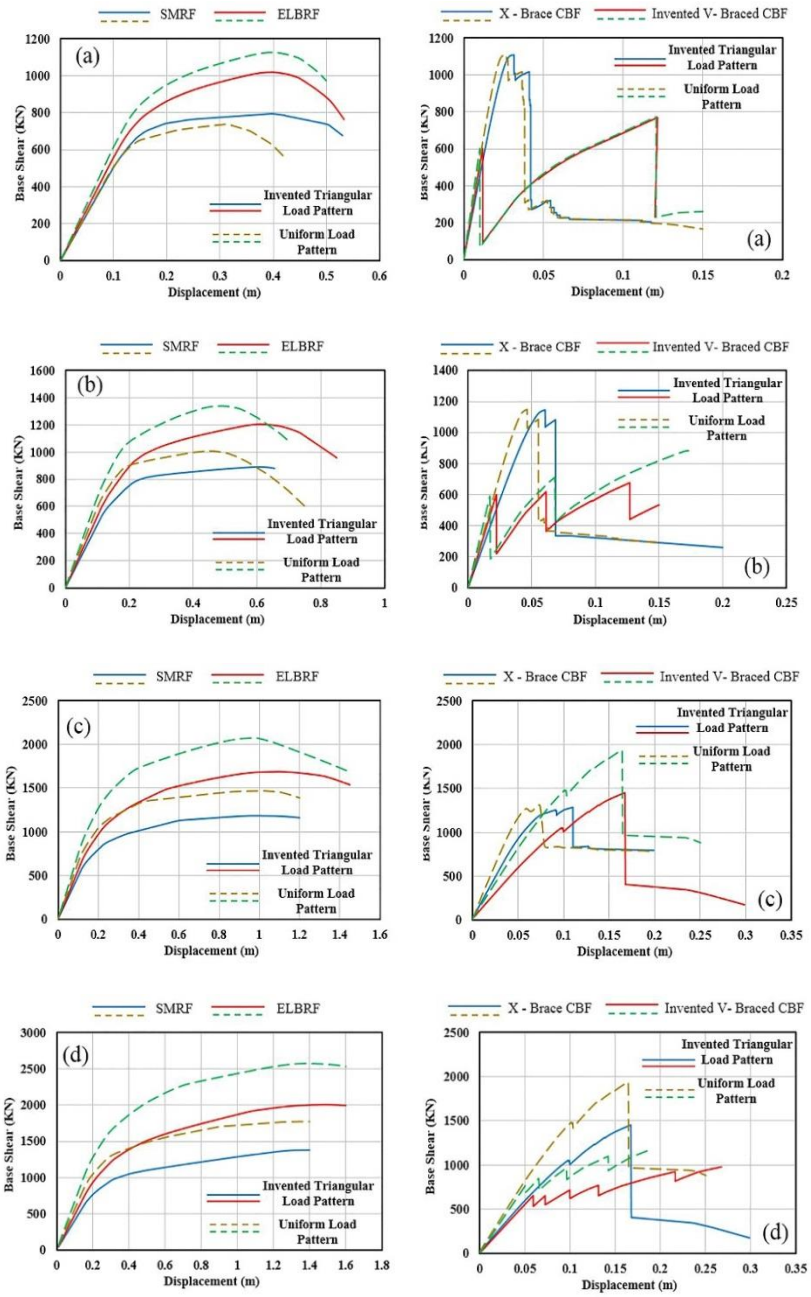

Fig. 10. Pushover curves of studied frames for Inverted triangular and Uniform load patterns in SMRF, X- Braced CBF, Inverted V- Braced CBF and ELBRF in a) 3-Story, b) 5-Story, c) 7-Story, d) 10-Story.

Table 6. First hinge base shear of the models for Inverted triangular load pattern and Uniform load pattern in SMRFs, X-braced CBFs, Inverted V-braced CBFs and ELBRFs.

No. of story	Vs (KN)							
	Inverted triangular load pattern				Uniform load pattern			
	SMRF	X-braced CBF	Inverted V - braced CBF	ELBRF	SMRF	X-braced CBF	Inverted V - braced CBF	ELBRF
3	436.00	586.20	118.09	561.01	413.95	592.74	106.85	495.25
5	530.89	578.24	253.65	556.30	504.34	600.92	284.09	635.33
7	557.72	637.14	504.03	836.96	717.97	614.95	723.22	991.78
10	608.20	701.84	303.41	931.31	842.17	731.09	425.47	1276.39

7.2. Evaluation of Conventional Pushover Procedures

According to the obtained results above and the description of the design method through the ultimate limit state and allowable stress methods, the ductility, overstrength factors and response modification factor are calculated for SMRF, X-Braced CBF, Inverted V-Braced CBF and ELBRF frames and the results are tabulated in Tables 7 – 10.

Table 7. Overstrength, ductility factors and response modification factor of model for Inverted triangular load pattern in X- Braced CBFs and Inverted V-braced CBFs.

No. of story	X-braced CBF						Inverted V -braced CBF					
	R_{SO}	R_S	Rμ	γ	R_{ASD}	R_{LRFD}	R_{SO}	R_S	Rμ	γ	R_{ASD}	R_{LRFD}
3	2.1	2.42	4.16	1.44	14.47	10.05	2.1	2.42	4.35	1.44	15.13	10.51
5	1.94	2.23	3.6	1.44	11.57	8.03	2.0	2.30	3.72	1.44	12.32	8.56
7	1.8	2.07	3.0	1.44	8.94	6.21	1.9	2.19	3.27	1.44	10.29	7.14
10	1.8	2.07	2.75	1.44	8.20	5.69	1.75	2.01	2.5	1.44	7.25	5.03

Table 8. Overstrength, ductility factors and response modification factor of model for Inverted triangular load pattern in SMRFs and ELBRFs.

No. of story	SMRFs						ELBRFs					
	R_{SO}	R_S	Rμ	γ	R_{ASD}	R_{LRFD}	R_{SO}	R_S	Rμ	γ	R_{ASD}	R_{LRFD}
3	2.15	2.47	4.65	1.44	16.56	11.50	2.28	2.62	5.1	1.44	19.26	13.37
5	1.95	2.24	3.86	1.44	12.46	8.66	2.1	2.42	4.36	1.44	15.16	10.53
7	1.85	2.13	3.15	1.44	9.65	6.70	2.0	2.30	3.4	1.44	11.26	7.82
10	1.8	2.07	2.82	1.44	8.41	5.84	2.0	2.30	2.97	1.44	9.84	6.83

Table 9. Overstrength, ductility factors and response modification factor of model for Uniform load pattern in X- Braced CBFs and Inverted V-braced CBFs.

No. of story	X-braced CBF						Inverted V -braced CBF					
	R_{SO}	R_S	Rμ	γ	R_{ASD}	R_{LRFD}	R_{SO}	R_S	Rμ	γ	R_{ASD}	R_{LRFD}
3	2.08	2.39	4.51	1.44	15.53	10.79	2.07	2.38	4.23	1.44	14.50	10.07
5	1.92	2.21	3.94	1.44	12.53	8.70	1.97	2.27	3.85	1.44	12.56	8.72
7	1.76	2.02	3.63	1.44	10.58	7.35	1.90	2.19	3.32	1.44	10.45	7.25
10	1.75	2.01	2.97	1.44	8.61	5.98	1.82	2.09	2.76	1.44	8.32	5.78

Table 10. Overstrength, ductility factors and response modification factor of model for Uniform load pattern in SMRFs and ELBRFs.

No. of story	SMRFs						ELBRFs					
	R_{SO}	R_S	Rμ	γ	R_{ASD}	R_{LRFD}	R_{SO}	R_S	Rμ	γ	R_{ASD}	R_{LRFD}
3	2.24	2.58	4.75	1.44	17.62	12.24	2.32	2.66	5.24	1.44	20.13	13.98
5	2.05	2.36	3.94	1.44	13.38	9.29	2.17	2.49	4.47	1.44	16.06	11.15
7	1.96	2.25	3.32	1.44	10.78	7.48	2.12	2.43	3.72	1.44	13.06	9.07
10	1.92	2.21	2.86	1.44	9.09	6.31	2.10	2.41	3.14	1.44	10.92	7.58

As observed the ductility, overstrength factors and response modification factor (subject to bracing configuration type) decrease as building height increase. Here, the changes in the overstrength and ductility factors for a distinctive type of bracing configuration indicate that, the ductility factor decreases more rapidly compared to the overstrength factor as the number of stories increase. Since the primary frames are designed based on the preliminary response modification factor and their empirical values

nce the primary frames are designed based on the preliminary response modification factor and their empirical values ber of stories increase.he overstrength tion factor the models are modified based on the newly modified respond factors and they are designed based on new response modification factors. Next, according to the mentioned method, all models are analyzed once more and their final seismic response modification factors are calculated.

7.3. Plastic Hinge Formation

The most important indicator in determining the damage level is to determine the number by which plastic hinges are distributed. In Open Sees software [26], beams and columns are modeled as elastic elements with a concentrated plastic hinge (CPH) at the end. Concentrated hinges are indicative of torsional springs the properties of which are yield from the complicated principles of mechanical engineering modified through strength curve and determination regulations of the modified Ibarra-Krawimkler model. During implementation of the lateral load to the structure step by step, the plastic hinges that exhibit non-elastic behavior at different levels are set at different performance levels which shown in colors indicating non-damage to complete degradation, Fig. 11.

Based on the idea of a secure chain, the structure has two reactive brittle and yieldable brittle rings. The brittle rings should be designed in a sense that when subject to seismic loads they can be released from the reactive zone following the soft ring in a manner, where the yield process is concentrated in the soft ring and the brittle ring will not be damaged. Thus, it can be assured that moment mechanism would be occurred during earthquake and the unpleasant failure will be prevented in the hinges and members.

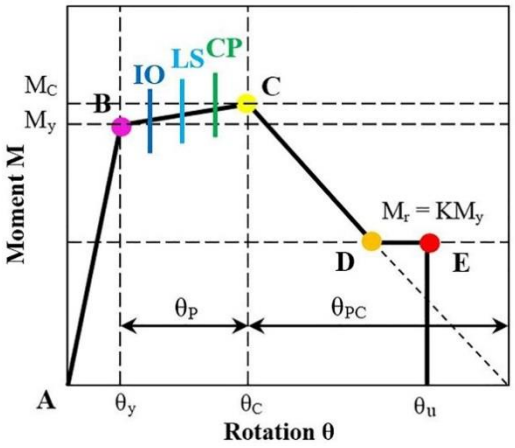

Fig. 11. Monotonic Moment-Rotation correlation for the modified Ibarra−Medina−Krawinkler deterioration model [40].

According to the formation of plastic hinges in ELBRF frames, subject to inverted triangular load and uniform load patterns it is revealed that, first, the elliptic braces enter the plastic zone, reach rupturing state and absorb the energy thereof. As to the ELBRF frames, unlike other frames, the column in the upper floors become more vulnerable to collapse as the number of stories increase. This fact prevents the failure of the columns in the lower floors, thus, preventing early structure destruction.

The results obtained from formation of plastic hinges in an NSPA method subject to inverted triangular load pattern and uniform load pattern in the last step in ELBRFs are presented in Figures 12 and 13 in drawings.

7.4. Target Displacement Evaluation

The target displacements applicable in FEMA-356 [13] is a decisive method in estimating the maximal displacement of the roof for each one of the SMRFs, X-braced CBFs, Inverted V-braced CBFs, and ELBRFs

structures based on different lateral load patterns, Tables 11 and 12.

Table 11. Target Displacement Evaluation (unit: m).

No. of Story	SMRFs			X-braced CBF			Inverted V-braced CBF			ELBRF		
	Inverted Triangular	Uniform	Mode One	Inverted Triangular	Uniform	Mode One	Inverted Triangular	Uniform	Mode One	Inverted Triangular	Uniform	Mode One
3	0.141	0.122	0.138	0.08	0.074	0.076	0.0907	0.086	0.09	0.188	0.178	0.179
5	0.173	0.158	0.177	0.135	0.12	0.13	0.125	0.115	0.12	0.207	0.195	0.201
7	0.184	0.171	0.181	0.155	0.136	0.14	0.155	0.145	0.15	0.235	0.226	0.228
10	0.216	0.214	0.20	0.165	0.14	0.145	0.24	0.184	0.194	0.276	0.264	0.266

Table 12. Target Displacement Evaluation in Modal Pushover Analysis (unit: m).

Frame	SMRFs			X-braced CBF			Inverted V-braced CBF			ELBRF		
No. Mode	1	2	3	1	2	3	1	2	3	1	2	3
3-Story	0.18	0.042	0.02	0.098	0.009	0.0026	0.11	0.011	0.004	0. 223	0.084	0.05
5-Story	0.22	0.063	0.03	0.148	0.03	0.0077	0.16	0.022	0.005	0.276	0. 115	0.072
7-Story	0.29	0.102	0.045	0.20	0.042	0.0013	0.207	0.038	0.011	0.36	0.16	0.086
10-Story	0.32	0.14	0.051	0.220	0.055	0.0151	0.265	0.06	0.025	0.394	0.187	0.095

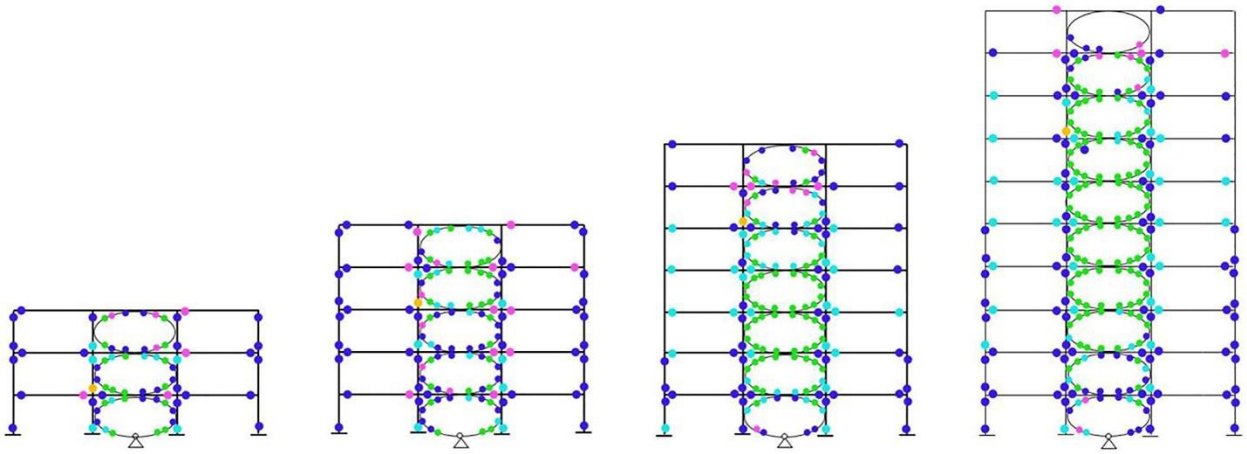

Fig. 12. The formation of plastic hinges subject to inverted triangular load pattern for ELBRFs in a) 3-story, b) 5- story, c) 7-story and d) 10-story.

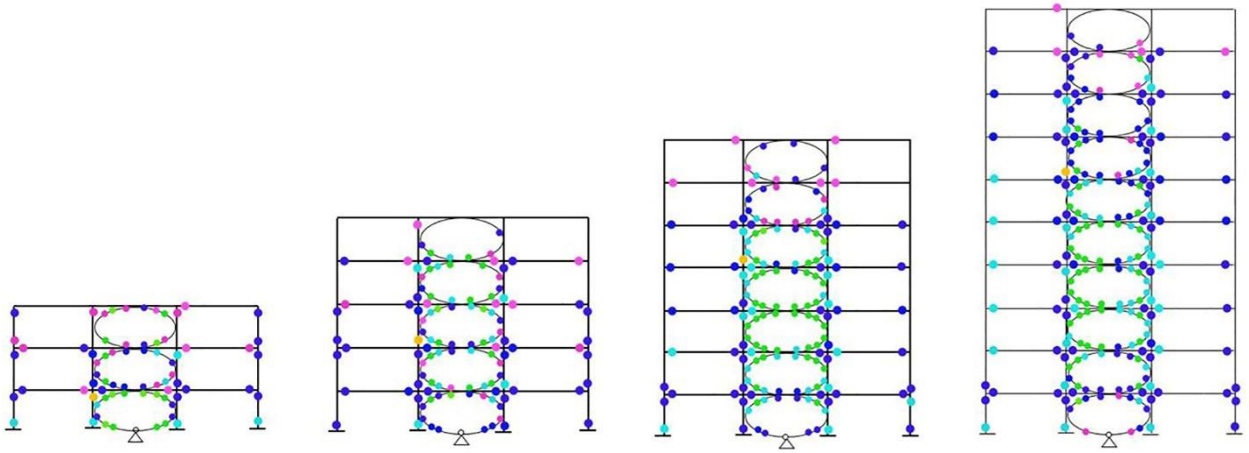

Fig. 13. The formation of plastic hinges subject to uniform load pattern for ELBRFs in a) 3-story, b) 5- story, c) 7-story and d) 10-story.

8. Conclusions

In this paper, ductility, overstrength factors and response modification factor and the process of forming plastic hinges for ELBRF are evaluated subject the inverted triangular load pattern and uniform load pattern by running nonlinear static analysis.

The following results, are briefed in bullets are as follows:

- Overstrength and ductility factors decrease with an increase in the number of stories.

- The overstrength factor for ELBRF subject to inverted triangular load pattern and uniform load pattern are 2.4 and 2.5 respectively.

- The ductility factors ELBRF subject to inverted triangle load pattern and uniform load pattern are 4.0 and 4.15 respectively.

- Response modification factors for ELBRF in the allowable stress design method subject to inverted triangular load pattern and uniform load pattern are 13.88 and 15.0 respectively.

- Response modification factors for ELBRF in the limit state design method subject to inverted triangular load pattern and uniform load pattern are 9.6 and 10.5 respectively.

- In general, the overstrength factor and the force reduction factor derived from ductility for the ELBRF are recommended as 2.45 and 4.1, respectively.

- The response modification factor for ELBRF is proposed for both design methods (ultimate limit state and allowable stress methods) as 10 and 14.4, respectively.

- By comparing the pushover diagrams in the SMRF and ELBRF structures for both the inverted triangular load and the uniform load patterns, the structural stiffness in ELBRFs grows 25% in average and the structural behavior in the nonlinear region faces considerable change.

- According to plastic hinge formation trend in ELBRF frames, elliptic braces were firstly entered into the plastic zone and collapsed finally which greatly contribute to energy absorption. In ELBRF frames, unlike other frames, the columns of upper stories collapse by an increase in the number of stories.

REFERENCES

[1] Krawinkler H, Seneviratna G. (1998). Pros and cons of a pushover analysis of seismic performance evaluation. Engineering structures, 20: 452-464.

[2] Shoeibi S, Kafi M.A, MajidGholhaki. New performance-based seismic design method for structures with structural fuse system. Engineering Structures 132 (2017) 745–760.

[3] Dipti R. Sahoo, Shih-Ho Chao. Performance-based plastic design method for buckling-restrained braced frames, Engineering Structures 32 (2010) 2950–2958.

[4] Zhifeng Liu, Sez Atamturktur, C. Hsein Juang. Performance based robust design optimization of steel moment resisting frames, Journal of Constructional Steel Research 89 (2013) 165–174.

[5] H. Moghaddam, I. Hajirasouliha. An investigation on the accuracy of pushover analysis for estimating the seismic deformation of braced steel frames. Journal of Constructional Steel Research 62, 2006: 343–351.

[6] N. Fanaie, S. Ezzatshoar, Studying the seismic behavior of gate braced frames by incremental dynamic analysis (IDA), Journal of Constructional Steel Research 99 (2014) 111–120.

[7] Ehsan Fereshtehnejad. E, Mehdi Banazadeh, Abdollah Shafieezadeh. System reliability-based seismic collapse assessment of steel

moment frames using incremental dynamic analysis and Bayesian probability network. Engineering Structures 118; 2016: 274–286.

[8] Djamal Yahmi, Taïeb Branci, Abdelhamid Bouchaïr, Eric Fournely. Evaluation of behaviour factors of steel moment-resisting frames using standard pushover method, Volume 199, 2017, Pages 397-403.

[9] Longo A., Montuori R., Piluso V. Plastic design of seismic resistant V-braced frames. Journal of Earthquake Engineering, Vol. 12, Issue 8, 2008, p. 1246-1266.

[10] Ghasemi J.H, Haghollahi A, Moghaddam H, Sarvghad Moghadam A.R. Study of the seismic performance of steel frames in the elliptic bracing. JVE International LTD. Journal of Vibroengineering. Aug 2016, vol. 18, Issue 5. ISSN 1392-8716.

[11] BHRC. Iranian code of practice for seismic resistance design of buildings: standard no. 2800. 4rd ed. Building and Housing Research Center; 2013.

[12] MHUD. Iranian National Building Code, part 10, steel structure design. Tehran (Iran): Ministry of Housing and Urban Development; 2013.

[13] FEMA 356, American Society of Civil Engineers. Prestandard and commentary for the seismic rehabilitation of buildings. Washington (DC): Federal Emergency Management Agency; 2000.

[14] Saravanan M, Arul Jayachandran S, Marimuthu V, Prabha P. Advanced analysis of cyclic behaviour of plane steel frames with semi-rigid connections. Steel and Composite Structures, Vol. 9, Issue 4, 2009, p. 381-395.

[15] Chou C. C., Tsai K. C., Wang Y. Y., Jao C. K. Seismic rehabilitation performance of steel side plate moment connections. Earthquake Engineering and Structural Dynamics, Vol. 39, 2010, p. 23-44.

[16] Hsu H. L., Tsao J. W. Flexural–torsional performance of thin-walled steel hollow box columns subjected to a cyclic eccentric load. Thin-Walled Structures, Vol. 45, Issue 2, 2007, p. 149-158.

[17] Sh.Hosseinzadeh, B.Mohebi. Seismic evaluation of all-steel buckling restrained braces using finite element analysis, Volume 119, March 2016, Pages 76-84.

[18] Yoo JH, Lehman DE, Roeder CW. Influence of connection design parameters on the seismic performance of braced frames. J Constr Steel Res 2008;64(6):607–23.

[19] FEMA 273. NEHRP guidelines for the seismic rehabilitation of buildings. Federal Emergency Management Agency; 1997.

[20] Krawinkler H, Seneviratna GDPK. Pros and cons of a pushover analysis of seismic performance evaluation. Engineering Structures 1998;20(4–6):452–64.

[21] Gupta B, Kunnath SK. Adaptive spectra-based pushover procedure for seismic evaluation of structures. Earthquake Spectra 2000;16(2): 367–92.

[22] Chopra AK, Goel R. A modal pushover analysis procedure for estimating seismic demands for buildings. Earthquake Engineering and Structural Dynamics 2002;31: 561–82.

[23] Anil K. Chopra and Rakesh K. Goel. Evaluation of Modal and FEMA Pushover Analyses: SAC Buildings. Journal of Earthquake Spectra, Volume 20, No. 1, pages 225–254, February 2004.

[24] Uang CM. Establishing R or (Rw) and Cd factor building seismic provision. J Struct Eng. 1991; 117 (1):19–28.

[25] Uniform building code. Whitter, California: International Conference of Building Officials; 1997.

[26] Mazzoni S, McKenna F, Scott MH, Fenves GL, Jeremic B. Opensees command language manual; 2013.

[27] Ibarra, L. F., and Krawinkler, H. (2005). “Global collapse of frame structures under seismic excitations,” Technical Report 152, The John A. Blume Earthquake Engineering Research Center, Department of Civil Engineering, Stanford University, Stanford, CA. [electronic version: https://blume.stanford.edu/tech report].

[28] Yun SY, Hamburger RO, Cornell CA, Foutch DA. Seismic performance for steel

moment frames. ASCE J Struct Eng 2002;128(4).

[29] Krawinkler H. State of art report on systems performance of moment resisting steel frames subject to earthquake ground shaking. SAC report no. 355C. Washington (DC): FEMA; 2000.

[30] Ibarra, L.F., Medina, R.A., and Krawinkler, H., 2005, "Hysteretic models that incorporate strength and stiffness deterioration," International Journal for Earthquake Engineering and Structural Dynamics, Vol. 34, No.12, pp. 1489-1511.

[31] FEMAP-695. Quantification of seismic performance factors. FEMAP-695 Report, prepared by the Applied Technology Councilfor the Federal Emer- gency Management Agency, Washington, DC;2009.

[32] Lignos, D. G., and Krawinkler, H. (2011). "Deterioration Modeling of Steel Beams and Columns in Support to Collapse Prediction of Steel Moment Frames," ASCE, Journal of Structural Engineering, Vol. 137 (11), 1291-1302.

[33] Lignos, D.G., and Krawinkler, H., 2007, "A database in support of modeling of component deterioration for collapse prediction of steel frame structures," ASCE Structures Congress, Long Beach, California.

[34] Ibarra LF, Medina RA, Krawinkler H. Hysteretic models that incorporate strength and stiffness deterioration. Earthquake Eng Struct Dyn 2005;34(12):1489–511.

[35] Lignos, D.G., Sidesway collapse of deteriorating structural systems under seismic excitations, Ph.D. Dissertation, Department of Civil and Environmental Engineering, Stanford University, Stanford, CA, 2008.

[36] Lignos, D. G., and Krawinkler, H. Dimitrios G. "Deterioration Modeling of Steel Components in Support of Collapse Prediction of Steel Moment Frames under Earthquake Loadin," Journal of Structural Engineering, 2011, 137(11): 1291-1302.

[37] Ali Pourgharibshahi, Touraj Taghikhany. Reliability-based assessment of deteriorating steel moment resisting frames. Journal of Constructional Steel Research 71, 2012: 219–230.

[38] PEER/ATC-72-1. Modeling and Acceptance Criteria for Seismic Design and Analysis of Tall Buildings, 2010.

[39] D.G. Lignos, H. Krawinkler and F. Zareian. Modeling of component deterioration for collapse prediction of steel moment frames. Conference: STESSA August 2009: Behaviour of Steel Structures in Seismic Areas, At Lehigh University, Pennsylvania, USA, Volume: 1.

[40] Junwon Seo, Jong Wan Hu and Burte Davaajamts. Seismic Performance Evaluation of Multistory Reinforced Concrete Moment Resisting Frame Structure with Shear Walls. Journal of sustainability. October 2015, vol. 7, Issue 5. ISSN 2071-1050.